USING HYPERSPECTRAL DATA FOR URBAN BASELINE STUDIES, BOULDER, COLORADO

F. A. Kruse[1]
J. W. Boardman[2]

And K. E. Livo[3]

1.0 Introduction

This study represents preliminary efforts towards establishing hyperspectral analysis approaches and methods for use in urban environments. The focus of this initial effort is the analysis of Airborne Visible/Infrared Imaging Spectrometer (AVIRIS) data acquired 14 October 2003 for Boulder, Colorado. While 11 flightlines covering Boulder were acquired, only the two flightlines covering the center portion of the city were analyzed for this study. F03101401p00r08 (Run 08), was collected with approximately 3.8m spatial resolution and F03101401p00r10 (Run 10), covering the same core area, has approximately 0.7m spatial resolution in the cross track direction. It is, however, undersampled by an approximate factor of 5 in the down track (flightline) direction. We applied model-based atmospheric correction algorithms to the data to produce surface scaled reflectance followed by analysis using the "standardized" approach developed by Analytical Imaging and Geophysics, LLC (AIG). Spectral endmembers were extracted from the AVIRIS data for selected sites and reconnaissance mapping was conducted using both the Spectral Angle Mapper (SAM) approach and partial unmixing (Mixture-Tuned-Matched-Filtering – MTMF). We also compiled endmember spectra into spectral libraries for additional validation and future use. We were able to successfully use endmember spectra from Run 08 to map Run 10 and visa versa. We also used a USGS library of synthetic materials to do direct material mapping. Orthorectification of the two datasets was used to allow direct comparison of spectral mapping at the two different pixel sizes. The mapping results demonstrate that the methods developed primarily for geologic mapping are generally applicable to urban environments. The complexity of these areas, however, will require modification and refinement of the methods. The methodology, mapping results, and some recommendations for mapping refinements are presented.

2.0 Background

Imaging Spectrometry data or Hyperspectral Imagery (HSI) measure the reflectance or emissivity of the Earth's surface in many spectral bands, providing both spatial images, and contiguous spectral coverage over selected spectral ranges (Goetz et al., 1985). HSI data acquired using airborne systems have been used in the geologic community since the early 1980's. The solar spectral range, 0.4 to 2.5 micrometers, provides abundant information about many important Earth-surface minerals (Clark et al., 1990) and research has proven the ability of hyperspectral systems to uniquely identify and map many of these minerals, even in sub-pixel abundances (Goetz et al., 1985, Kruse and Lefkoff, 1993, Boardman and Kruse, 1994; Kruse et al., 1999; Clark et al., 2003, Kruse et al., 2003). Research has shown that imaging spectrometry principles and mapping capabilities are extensible to many other disciplines. Limited work has been done with hyperspectral analysis of the Urban Environment – the topic of this study (Heiden,

[1] Horizon GeoImaging, LLC, 4845 Pearl East Circle, Suite 101, Boulder, CO 80303-6113 USA, kruse@hgimaging.com, http://www.hgimaging.com

[2] Analytical Imaging & Geophysics, LLC (AIG), Boulder, Colorado

[3] U. S. Geological Survey, Denver, Colorado

2001; Marino et al, 2001; Fiumi, 2001). One of the limiting factors in many of these studies (and specifically for the Urban Environment) is the absence of adequate spectral libraries and baseline studies of the spectral characteristics and spectral/spatial variability of specific materials of interest. This study is designed as an initial investigation into spectral characterization and mapping of the Urban Environment. The principal objective of this work was to establish a preliminary Hyperspectral Mapping Baseline for urban areas by evaluating and demonstrating existing hyperspectral analysis approaches using AVIRIS data of Boulder, Colorado. Additional objectives were to validate and refine hyperspectral mapping capabilities through collection of a site-specific spectral library utilizing a field spectrometer and/or spectra from the AVIRIS data.

3.0 Approach

Our approach to analysis of these data was to utilize model-based atmospheric correction methods and existing HSI data analysis methods available in the commercial off-the-shelf (COTS) software package "ENVI" (The Environment for Visualizing Images) to establish baseline mapping capabilities using HSI data of urban areas. We selected the city of Boulder, Colorado and surrounding areas as the primary test site for this investigation and as an initial analog for urban areas in general. This allows us to conduct field verification efforts with minimal cost. While the analyzed data are specific to the Boulder Urban area, absolute reflectance correction of the AVIRIS data, collection of AVIRIS endmember spectra, and measurement of additional spectra of key materials utilizing a USGS-provided Analytical Spectral Devices (ASD) spectrometer allow establishment of prototype spectral libraries/databases for potential use in other urban areas. The following summarizes the approaches used for analyses of these data.

3.1 Atmospheric Correction

Atmospheric correction is a requirement for this data analysis approach. We used the Atmospheric COrrection Now (ACORN) model-based atmospheric correction method in this study. ACORN is a commercially-available, enhanced atmospheric model-based software that uses licensed MODTRAN4 technology to produce high quality surface reflectance without ground measurements (Kruse, 2004). Field spectra measured for targets occurring in the HSI data were also used to refine the atmospheric correction..

3.2 Standardized "Hourglass" HSI Data Analysis

Standardized approaches developed by the 1st author (Kruse) and associates at Analytical Imaging and Geophysics LLC (AIG) for analysis of HSI data (Boardman et al, 1995; Kruse et al., 1997) are implemented and documented within the "Environment for Visualizing Images" (ENVI) software system (now a Research Systems Inc [RSI] commercial-off-the-shelf [COTS] product) (Research Systems Inc, 2003) (Figure 1).

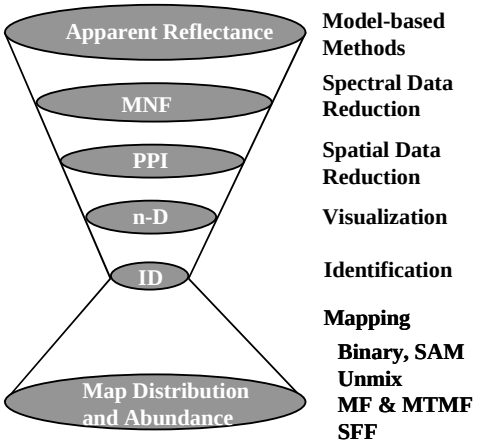

Figure 1: The "Hourglass" HSI analysis approach.

A key point of this methodology is the reduction of data in both the spectral and spatial dimensions to locate, characterize, and identify a few key spectra (endmembers) in the HSI data that can be used to explain the rest of the hyperspectral dataset. Once these endmembers are selected, then their location and abundances can be mapped from the linearly-transformed or original data. These methods derive the maximum information from the hyperspectral data themselves, minimizing the reliance on a priori or outside information. The analysis approach consists of the following steps:

1. Correction for atmospheric effects using an atmospheric model such as ACORN (AIG, 2001)
2. Spectral compression, noise suppression, and dimensionality reduction using the Minimum Noise Fraction (MNF) transformation (Green et al., 1988; Boardman, 1993),
3. Determination of endmembers using geometric methods (Pixel Purity Index – "PPI") (Boardman et al., 1994, 1995)
4. Extraction of endmember spectra using n-dimensional scatter plotting (Boardman et al., 1995)
5. Identification of endmember spectra using visual inspection, automated identification, and spectral library comparisons (Kruse and Lefkoff, 1993; Kruse et al., 1993a)
6. Production of material maps using a variety of mapping methods. The "Spectral Angle Mapper" (SAM) produces maps of the spectrally predominant mineral for each pixel by comparing the angle between the image spectra and reference spectra in n-dimensional vector space (Kruse et al., 1993b). "Mixture-Tuned-Matched-Filtering" (MTMF) is basically a partial linear spectral unmixing procedure (Boardman, 1998).

The Hourglass method described above is not the only way to analyze hyperspectral data, but we have found that it provides a consistent way to extract spectral information from hyperspectral data without a priori knowledge or requiring ground observations. The individual steps are described in more detail in (Kruse et al., 1997 and Kruse, 2003).

3.3 Spectral Libraries

The above methods assume that the key spectral elements will be extracted from the HSI data themselves. As is often the case, if field or laboratory spectra of materials of interest have already been collected, these can be used to directly map the materials present by entering the Hourglass processing scheme at the neck – utilizing already-identified spectra and proceeding directly to Spectral Mapping. The USGS provided a draft (prototype) spectral library of "synthetic" materials for use on this project. The procedure for using these spectra for mapping involves resampling them to the AVIRIS wavelength response, transforming them and the data using the same MNF transform parameters, and applying MTMF spectral mapping.

One of the additional goals of this research is to begin establishing spectral libraries and/or databases of common urban materials for future use in HSI mapping of different areas. Because of the relatively short deadline of this project, the majority of these spectra are necessarily from the hyperspectral data themselves – key materials located during the hourglass analysis. Field reconnaissance was used to verify the identity of selected mapped materials and limited field verification spectral measurements were made. Spectra were compiled into ENVI-compatible libraries and prospective database elements were identified.

3.4 Orthorectification

Hyperspectral data can not truly be useful unless they are accurately map-referenced. JPL provided both "raw" flightline data and geocorrected data for the purposes of this research. The distorted nature of typical raw low-altitude AVIRIS imagery demands a thorough and accurate geolocation process. Analtyical Imaging and Geophysics, LLC (AIG) has provided all the geocorrection support for the JPL AVIRIS team since they first installed the C-MIGITS DGPS-IMU system in 1998 (Boardman, 1999).

Even so, the geocorrected data provided by JPL are really only a "first-cut" type correction. As part of this research, AIG further refined the AVIRIS geocorrection using a full orthorectification model. This provides the spatially accurate data we need both to locate specific spectral targets on the ground, and to compare HSI and other data at various spatial resolutions.

3.5 Field Verification

Because of the short duration of this project, only limited field verification was possible. Field spectral measurements were made by the PI and USGS personnel (Eric Livo) on the day of the AVIRIS overflight (14 October 2003) using an ASD Field Spectrometer. Additionally, visual reconnaissance was conducted on-site for a selection of spectrally unique materials determined from the AVIRIS data.

4.0 Results

AVIRIS data were originally delivered as geocorrected, calibrated radiance data. All initial atmospheric corrections and analyses described here for these data were performed on the geocorrected data. While we prefer to work with the non-geocorrected data for our spectral analyses, the non-geocorrected data and the information to perform basic geocorrection were delivered towards the end of the project, thus only limited studies were performed using the non-geocorrected data. We did use them for the orthorectification studies.

4.1 Assessment of "Standard" Analysis Methods

The "standard" methods described above were run on the Run 08 and Run 10 ACORN atmospherically corrected data to determine the feasibility of using them for characterizing and mapping urban environments using HSI data. Initial reconnaissance analyses were made on the full flightline data for Run 8. Typically for geologic work we divide each flightline into two spectral segments, the 0.4 – 1.3 micrometer (VNIR) and 2.0 –2.5 micrometer (SWIR) regions. The VNIR region allows separation of vegetation from geology and the mapping of iron-bearing minerals such as hematite, goethite, and jarosite. The SWIR region allows mapping of clays, carbonates, and other materials with vibrational molecular signatures (Clark et al., 1990). Many similar materials are found as components of the landscape and as building materials in urban areas, thus we initially pursued a similar approach for these data. Additional efforts were made to use the "combined" or full spectral range for these data, as we expected that many of the materials present in the urban environment might have unique components in both the VNIR/SWIR.

Using the standard approach for analysis of these data presents some problems not present in most geologic data sets. First, because only the geometrically corrected data were initially available for analysis, and the small pixel sizes (~4 and ~1m respectively for Run 8 and Run 10) the size of the dataset (1 Gb and 8 Gb respectively for the geocorrected Run 8 and Run 10 data) results in long execution times for the MNF and PPI stages of the analysis. Secondly, the high dimensionality of the dataset caused by high spectral variability in the urban environment greatly increases the complexity of the data as compared to geologic datasets and makes analysis using spectral mixing models difficult. For purposes of simplification of this report, only approximately the first 20 endmembers are reported here for each full-scene case. Additionally, we only used the Spectral Angle Mapper (SAM) mapping algorithm on the full flightline data – again to reduce complexity when mapping in reconnaissance mode. SAM is really only a first-cut spectral matching method, and has known performance (accuracy) limitations. Normally, we would use a mapping method such as "Mixture-Tuned-Matched-Filtering" (MTMF), but because of the time constraints and initial (exploratory) nature of this research, have only applied this method to the smaller (subset) data described below.

Two cases are reported below for the full flightline for Run 08 – 1) VNIR analysis, 2) SWIR analysis. These are first-cut reconnaissance/exploratory mapping efforts. The complexity of the data points out that, while running these programs on the whole dataset is possible, it seems that image

subsetting and/or segmentation is probably required to reduce the dimensionality and make analysis using these methods more feasible.

4.1.1 Run 8 - VNIR: Geometrically corrected data, 99 bands from 0.4 – 1.34 micrometers.
MNF was run on the VNIR only and bands 1-3, 33-35, 97 were excluded. (Wavelengths excluded 0.37 – 0.39, overlap at 0.65 – 0.67, 1.25 micrometers). Edges were masked for MNF. PPI was run on the first fifty (50) MNF bands. No edge masking was used for PPI because using a skip factor (every-other-pixel/every-other-line) was required (because of hardware memory limitations) and masking not allowed when skip factor used. Fifteen (15) selected Endmembers were extracted using the n-D Visualizer and were plotted (Figure 2) and used for spectral mapping. Table 1 describes the material interpretation for each of the selected endmembers. The Spectral Angle Mapper was used for initial, reconnaissance mapping to determine the locations of endmembers and show their spatial distribution for whole pixels only(Figure 2).

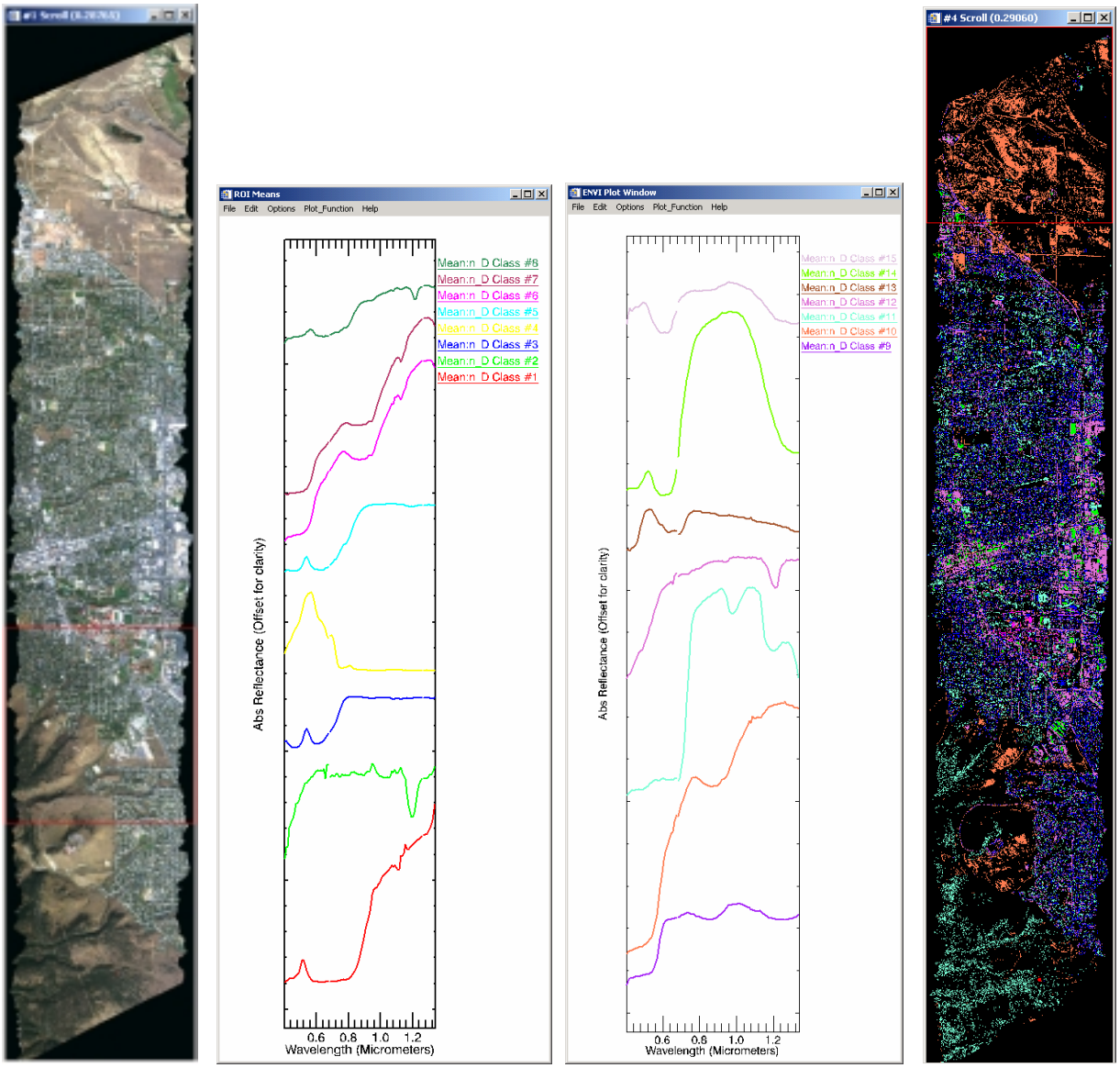

Figure 2: Endmembers extracted from the Run 8 VNIR data only. Left image is True Color composite. Endmember spectra are shown in center plots. Right image is SAM result with default thresholds.

Table 1: Full-Scene VNIR Endmembers – Interpretation based on spectral features and spatial context.

EM	Description
1	Unknown blue-green covering material on underground reservoir roof
2	Unknown roofing material with absorption feature near 1.2 micrometers
3	Vegetation #1 – along edges of non-vegetated areas?
4	Green water signature
5	Vegetation #2 ?
6	Red Tile Roofing Material #1
7	Red Tile Roofing Material #2
8	Vegetation-like material (Astroturf?)
9	Red Tile Roofing Material #3
10	Soil iron-oxide, some Red Tile Roofing Material
11	Healthy Green Vegetation
12	Asphalt and some roofing materials
13	Green material – Spruce municipal swimming pool?
14	Blue-green Vegetation-like man-made material #1 – occurs on one building
15	Blue-green Vegetation-line man-made material #2 – occurs on another bldg

4.1.2 *Run 8 - SWIR:* Geometrically corrected data, 50 bands from 2.02 – 2.5 micrometers.

MNF was run on the SWIR only and bands 107-112 and 150 – 174 were excluded (Wavelengths excluded 1.35-1.40, and 1.78 – 2.01 micrometers. Edges were masked for MNF. PPI was run on the first 25 MNF bands. No edge masking was used for PPI because using a skip factor (every-other-pixel/every-other-line) was required (because of hardware memory limitations) and masking not allowed when skip factor used. Nineteen (19) selected Endmembers were extracted using the n-D Visualizer and were plotted (Figure 3) and used for spectral mapping. Table 2 describes the material interpretation for each of the selected endmembers. The Spectral Angle Mapper was used for initial, reconnaissance mapping to determine the locations of endmembers and show their spatial distribution for whole pixels only(Figure 3).

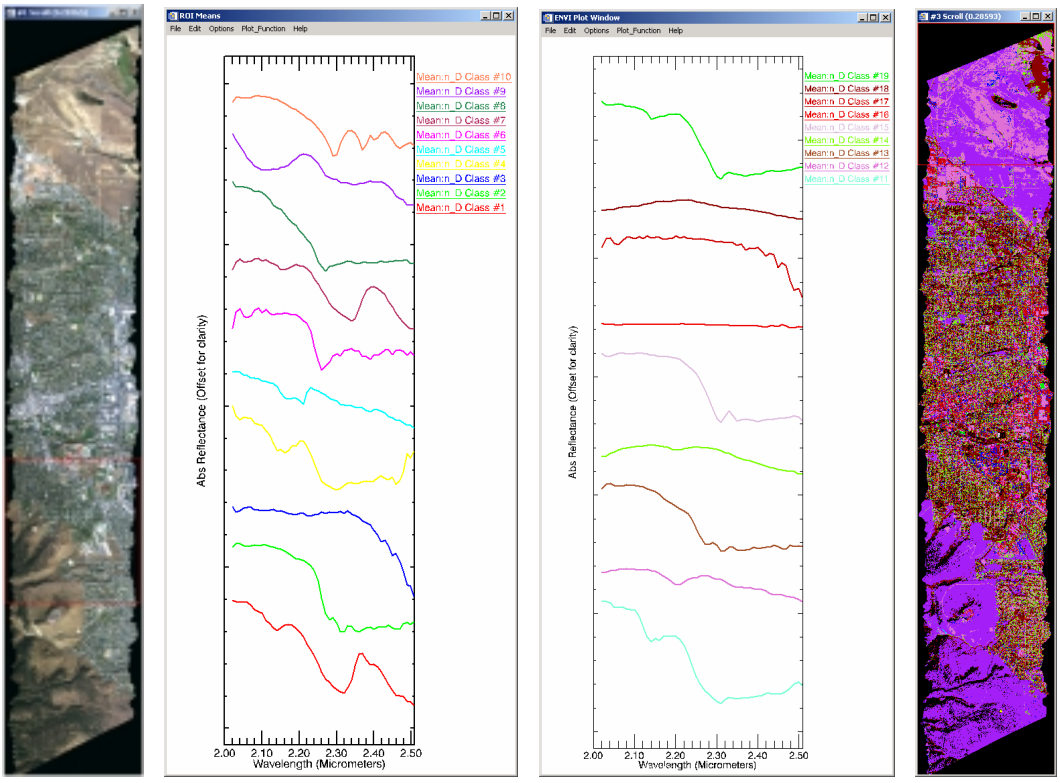

Figure 3: Endmembers extracted from the Run 8 SWIR data only. Left image is True Color composite. Endmember spectra are shown in center plots. Right image is SAM result with default thresholds.

Table 2: Full-Scene SWIR Endmembers – Interpretation based on spectral features and spatial context.

EM	Description
1	Calcite-bearing roofing material
2	Unknown roofing material with broad/flat absorption feature near 2.3 micrometers
3	Unknown material(s) with absorption "falloff" at long wavelengths
4	Water tank cover and one building roof (same as blue-green water tank)
5	Kaolinite occurring predominantly in natural exposures
6	Unknown roofing material with 2.26 micrometer absorption
7	Dolomite-Bearing Roofing Material
8	Unknown material with 2.27 micrometer absorption
9	Dry Vegetation signature, 2.1 and 2.3 absorptions, 2.2 micrometer peak
10	Unknown roofing material with 2.29 micrometer absorption
11	Unknown roofing material with 2.31 and 2.14 micrometer absorptions (1 bldg)
12	2.2 micrometer clay absorption feature
13	Roofing material with 2.27 micrometer aborption
14	Weak 2.2 micrometer clay absorption feature
15	Roofing material with 2.31 micrometer absorption (like 11 but no 2.14)
16	Flat signature – nothing mapped
17	Flat signature with falloff > 2.4 micrometers (ashphalt +?)
18	Green vegetation, with reflectance peak near 2.2 micrometers
19	Unknown roofing material with 2.31 and 2.14 micrometer absorptions

4.1.3 Reconnaissance Mapping with USGS-Provided spectral library

A spectral library of urban materials provided by the USGS was used to demonstrate an alternate method for basic reconnaissance mapping for the Run 08 (3.8m) data – using known spectra. The spectra were convolved to the 2003 AVIRIS wavelengths and used for both SAM and MTMF mapping. Endmembers selected were ones that should have been present in the Boulder, Colorado urban environment, including road materials (asphalt and concrete), several colors of asphalt shingles, two ages of cedar shingles, three colors of building bricks, and galvanized roofing material. Figure 4 shows selected library spectra and SAM mapping results for Boulder, Run 08.

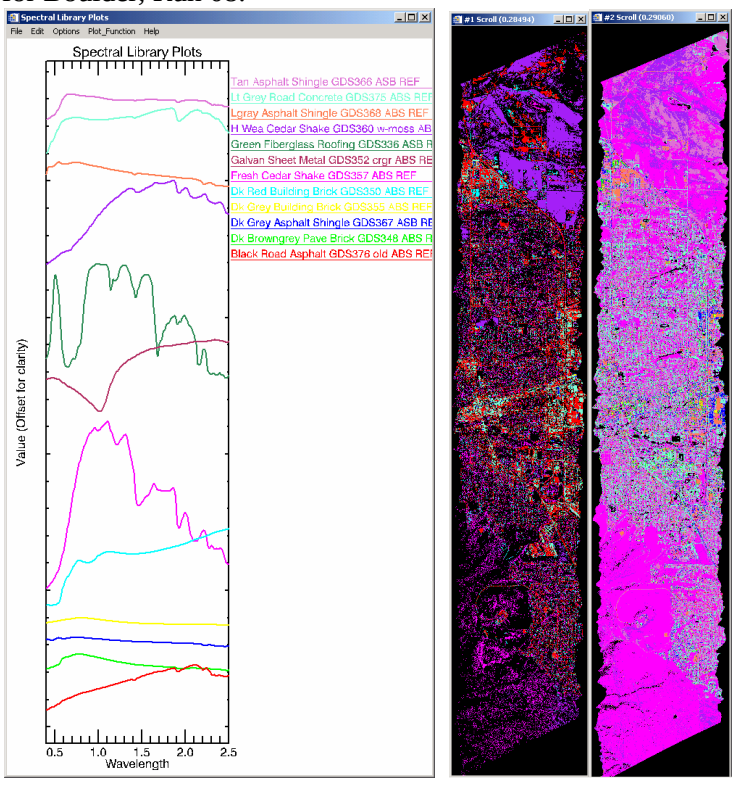

Figure 4: USGS Spectral Library reconnaissance mapping. Left – Selected library reference spectra. Center-VNIR SAM Mapping results. Right – SWIR SAM Mapping results.

4.1.4 *Analysis and Comparison of Spatial Subsets for Selected Areas*

We decided to look at two small spatial subsets in more detail because the large data volume for the two flightlines prohibited detailed analysis at this stage of the research. Both the VNIR and SWIR wavelength ranges were mapped using subset-specific MNF, PPI, and n-D Visualizer.

Run 08, Centennial Middle School, VNIR Analysis: MNF was run on the VNIR only for the Run 08 (3.8 meter) data and bands 1-3, 33-35, 97 were excluded. (Wavelengths excluded 0.37 – 0.39, overlap at 0.65 – 0.67, 1.25 micrometers). PPI was run on the first thirty-five (35) MNF bands for Run 08. Sixteen (16) selected Endmembers were extracted using the n-D Visualizer (only the best endmembers) and were plotted (Figure 5) and used for spectral mapping (Figure 6). Table 3 describes the material interpretation for each of the selected endmembers. SAM was used for reconnaissance, MTMF was used to better determine the locations of endmembers and show their abundance and spatial distribution (Figure 6).

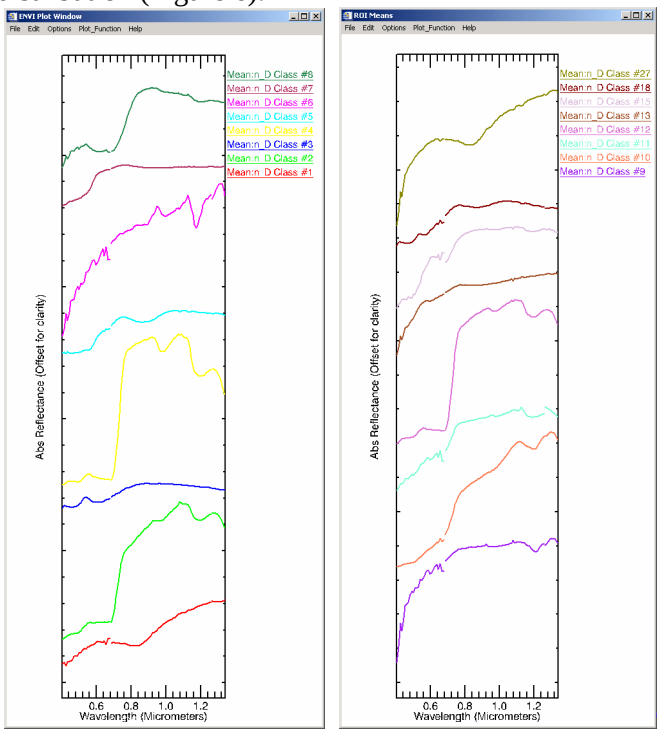

Figure 5: Line 9, Run08 Centennial Middle School Endmembers.

Table 3: Endmembers for the Line 9, Run 08 VNIR data for the Centennial Middle School site.

R08 VNIR Endmember	Description
1 (Red)	Building Roof #1- Fe Absorption
2 (Green)	Vegetation #1 (+-Dry Veg)
3 (Blue)	Green Tennis Court Surface #1
4 (Yellow)	Vegetation # 2 (Health = Healthiest)
5 (Cyan)	Red Tennis Court Surface
6 (Magenta)	Bare Soil #1
7 (Maroon)	Unknown (Roofing?) material
8 (Sea Green)	Unknown (Roofing?) material similar to green vegetation
9 (Purple)	Unknown roofing material
10 (Orange)	Dry vegetation?/Bare Soil
11 (Aquamarine)	Asphalt/bare soil
12 (Orchid)	Vegetation #3
13 (Sienna)	Concrete?/Bare Soil
15 (Thistle)	Yellow School Bus
18 (Red 3)	Mixed green and red tennis court surface
27 (Yellow 3)	Building Roof #2- Fe Absorption similar to EM#1

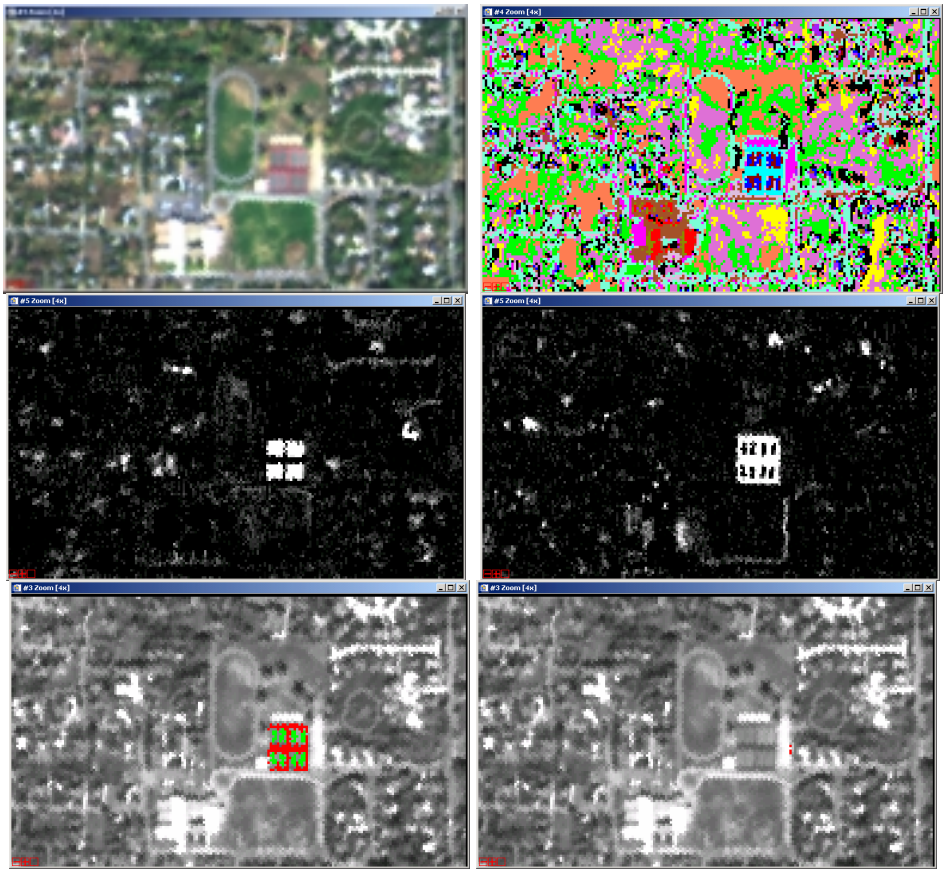

Figure 6: Top Left – Centennial Middle School subset true color composite. Top Right – SAM classification result. Middle Left: MF portion of MTMF for Green Tennis Court Endmember. Middle Right: MF portion of the MTMF for the Red Tennis Court Endmember. Bottom Left – MTMF mapping result for abundances greater than 10% for the Green and Red Tennis Court endmembers shown in their respective colors. Bottom Right: MTMF mapping results for Yellow School Bus endmember (3 pixels shown in red at right center of image).

Run 10, Centennial Middle School, VNIR Analysis: MNF was run on the VNIR only for Run 10 (0.7 meter spatial resolution) data and bands 1-5, 33-35, 77, and 97 were excluded (total of 96 bands used). (Wavelengths excluded 0.37 – 0.41, overlap at 0.65 – 0.67, single bands at 1.08 and 1.25 micrometers). PPI was run on the first thirty-five (35) MNF bands for Run 10. Eighteen (18) selected Endmembers were extracted using the n-D Visualizer (Figure 7). No effort was made to find all of the endmembers - only the best, most obvious endmembers were mapped. Table 4 describes the material interpretation for each of the selected endmembers. SAM was used for reconnaissance, MTMF was used to better determine the locations of endmembers and show their abundance and spatial distribution (Figure 8). Figure 9 shows a zoomed version of mapping for the "yellow school bus" endmember and a corresponding field photograph.

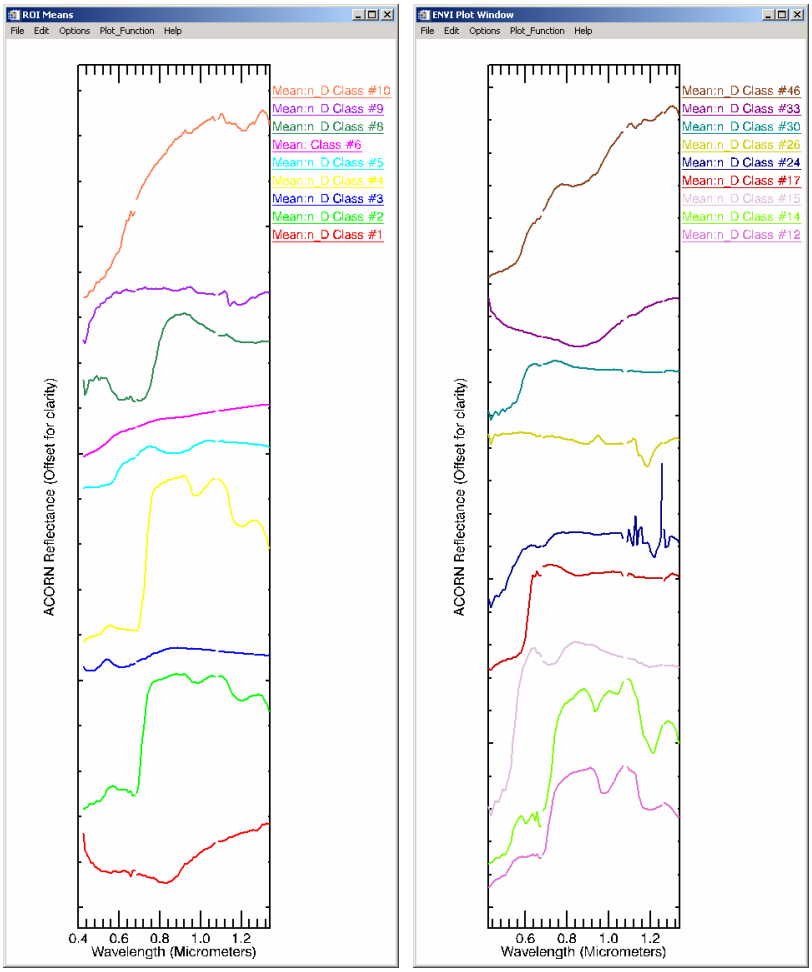

Figure 7: CMS VNIR Endmembers

Table 4: VNIR endmembers for the Line 9, Run 10 VNIR data for the Centennial Middle School site.

R08 VNIR Endmember	Description	R10 VNIR Endmember
1 (Red)	Building Roof #1- Fe Absorption	1
2 (Green)	Vegetation #1 (+-Dry Veg)	2
3 (Blue)	Green Tennis Court Surface #1	3
4 (Yellow)	Vegetation # 2 (Health = Healthiest)	4
5 (Cyan)	Red Tennis Court Surface	5
6 (Magenta)	Bare Soil #1	6
7 (Maroon)	Unknown (Roofing?) material	None
8 (Sea Green)	Unknown (Roofing?) material similar to green vegetation	8
9 (Purple)	Unknown roofing material	9
10 (Orange)	Dry vegetation?/Bare Soil	10
11 (Aquamarine)	Asphalt/bare soil	None
12 (Orchid)	Vegetation #3	12
13 (Sienna)	Concrete?/Bare Soil	13
None	Unknown – Vegetation-like signature	14
15 (Thistle)	Yellow School Bus	15
None	Red Vehicle Paint	17
18 (Red 3)	Mixed green and red tennis court surface	18
None	Unknown roofing?	24
None	Unknown Roofing material?	26
27 (Yellow 3)	Building Roof #2- Fe Absorption similar to EM#1	None
None	Unknown roofing material?	30
None	Unknown roofing material	33
None	Red roofing material?	46

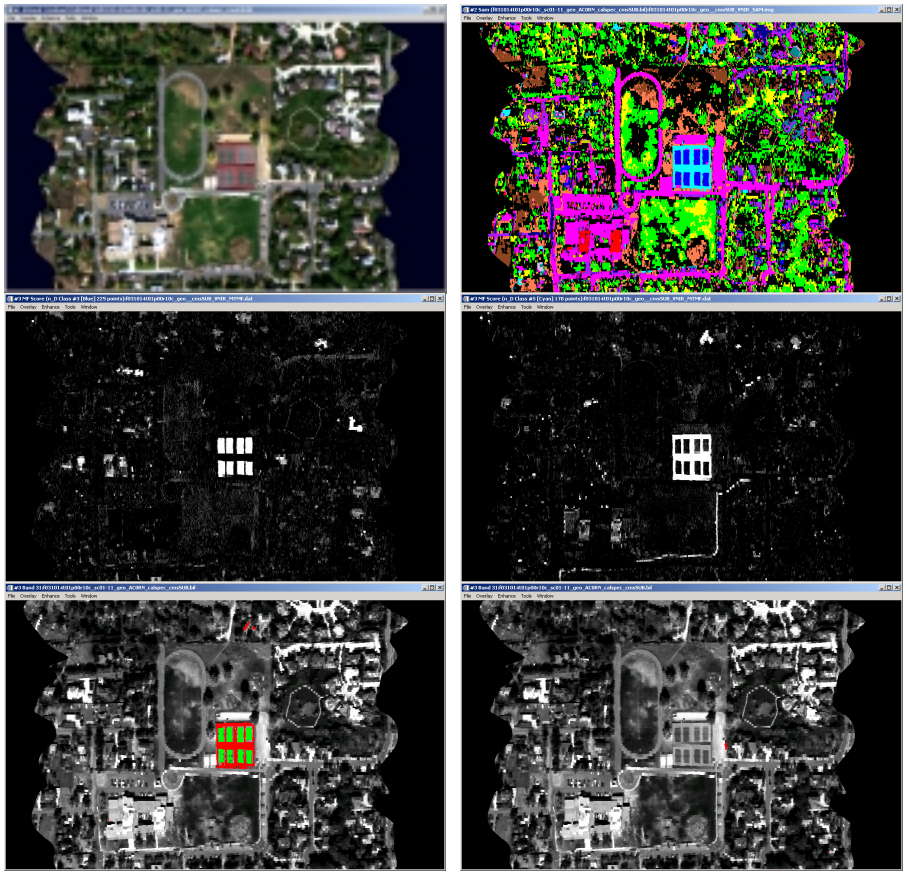

Figure 8: Top Left – Centennial Middle School subset true color composite. Top Right – SAM classification result. Middle Left: MF portion of MTMF for Green Tennis Court Endmember. Middle Right: MF portion of the MTMF for the Red Tennis Court Endmember. Bottom Left – MTMF mapping result for abundances greater than 10% for the Green and Red Tennis Court endmembers shown in their respective colors (note a few false alarms near top-center of image). Bottom Right: MTMF mapping results for Yellow School Bus endmember (Red Pixels at right center of image).

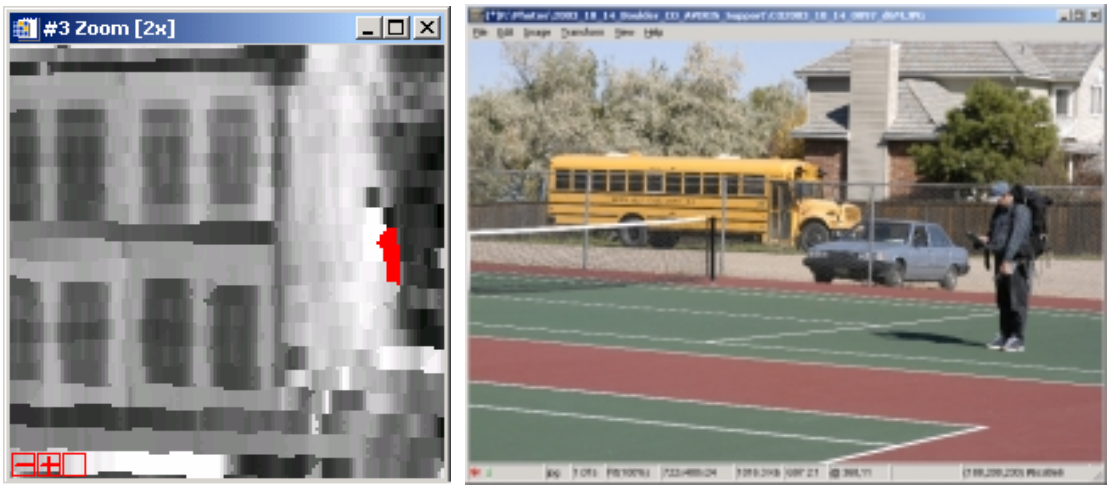

Figure 9: Left - Enlargement of portion of Centennial Middle School site showing location of yellow school bus highlighted in red from MTMF mapping. Right – Ground photo of yellow school bus with tennis courts in the foreground.

Run 10, Centennial Middle School, SWIR Analysis: Geometrically corrected data, 50 bands from 2.02 – 2.5 micrometers. MNF was run on the SWIR only and bands 107-112 and 150 – 174 were excluded (Wavelengths excluded 1.35-1.40, and 1.78 – 2.01 micrometers. Edges were masked for MNF. PPI was run on the first 15 MNF bands. Eleven (11) selected Endmembers were extracted using the n-D Visualizer and were plotted (Figure 10) and used for spectral mapping. Table 5 describes the material interpretation for each of the selected endmembers. The Spectral Angle Mapper was used for initial, reconnaissance mapping to determine the locations of endmembers and show their spatial distribution for whole pixels only (Figure 11). MTMF Mapping was not conducted.

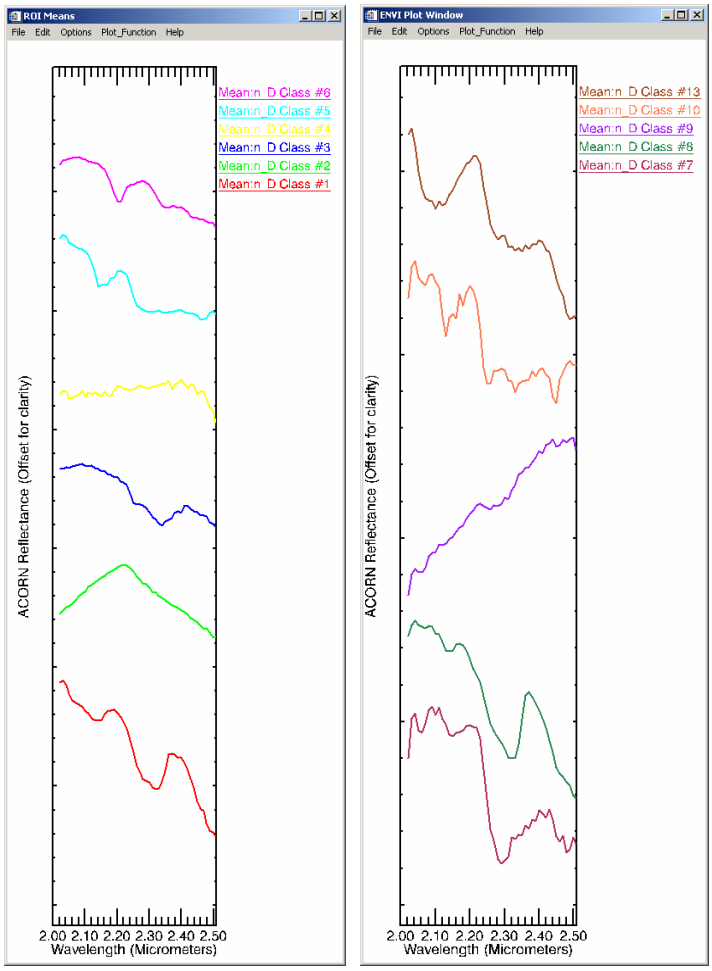

Figure 10: Run 10 CMS SWIR Endmembers

Table 5: Run 10 CMS SWIR Endmember Descriptions

Run 10 EM	Description
1	Carbonate – probably calcite
2	Green Vegetation
3	Chlorite
4	Asphalt/Asphalt Roofs?/Bare Soil (no absorption
5	Dry Vegetation?
6	Illite/Muscovite Soil Surface
7	Red Tennis Court Surface
8	Carbonate – Probably dolomite
9	Unknown Roof Surface
10	Unknown Roof Surface with multiple 2.1 - 2.3 micrometer absorptions
13	Dry Grass

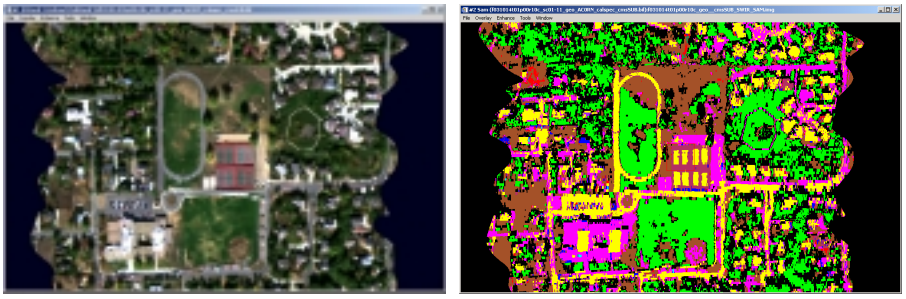

Figure 11: Left – True Color Composite. Right - Run 10 CMS SWIR mapping using SAM.

Run 08, Centennial Middle School, SWIR Analysis: Geometrically corrected data, 50 bands from 2.02 – 2.5 micrometers. MNF was run on the SWIR only and bands 107-112 and 150 – 174 were excluded (Wavelengths excluded 1.35-1.40, and 1.78 – 2.01 micrometers. PPI was run on the first 15 MNF bands. The n-D visualizer stage was not performed. Instead, the 13 endmembers located during the Run 10 CMS mapping (Figure 11) were used and SAM reconnaissance mapping was performed. Figure 12 shows the SAM mapping results. The similarity of the Run 10 SAM image map shown in Figure 11 and the Run 08 SAM image map in Figure 12 indicates that it is possible to use endmembers derived from one scene to map a scene acquired at a different time (and probably location as well). The prerequisite is that the data be well calibrated and have consistent reflectance corrections.

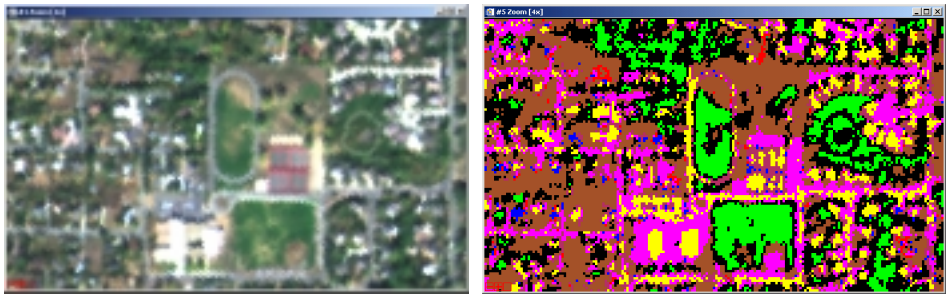

Figure 12: Left – True Color Composite. Right - Run 10 CMS SWIR mapping using SAM.

We also examined spatial issues related to platform instability and undersampling and modified, improved, and applied a full orthorectification procedure to both the Run 08 and Run 10 data. The orthorectified data show an approximately 5-fold improvement in registration accuracy over standard JPL geocorrection. The results of the process show that we can accurately geolocate each AVIRIS pixel to approximately +/- 1.5 pixels in position in well-sampled data and to approximately +/- 1.5 the downtrack sampling for highly undersampled data. The orthocorrection is important for future, more detailed analyses of the Boulder data as well as being applicable to other AVIRIS acquisitions in support of this study. We plan to leverage this orthocorrection capability heavily in subsequent work to allow direct comparison of the two different spatial resolutions and integration with high-spatial-resolution panchromatic and multispectral data as well as potentially examining multi-angle and multi-temporal urban hyperspectral exploitation schemes.

5.0 Discussion and Conclusions

We have outlined methods and analysis results for an initial, preliminary study directed towards establishing hyperspectral analysis approaches and methods for use in urban environments and recommending directions for future work. The focus of the initial effort was the analysis of AVIRIS data acquired 14 October 2003 for Boulder, Colorado. Two flightlines covering the center portion of the city were analyzed. Flightline 9, Run 08 was collected with approximately 3.8m spatial resolution and Flightline 9, Run 10, covering the same core area, has approximately 0.7m spatial resolution in the cross track direction. A model-based atmospheric correction was applied to the data to produce surface scaled reflectance. The reflectance data were analyzed using the standardized "hourglass" approach. Image-maps produced using these procedures successfully delineated areas of specific materials (vegetation, soils, urban elements), however, it was apparent from the analysis that further detail was available in the data that wasn't being extracted at the reconnaissance scale. It was also observed that the high dimensionality of the dataset caused by high spectral variability in the urban environment greatly increases the complexity of the data as compared to geologic datasets and makes analysis using spectral mixing models difficult. Even so, the mapping results demonstrated the basic feasibility of using existing HSI analysis methods to characterize and map urban environments. Additional work is required, however, to adequately determine the spectral characteristics of materials occurring in urban areas and to allow routine HSI mapping. Specific requirements identified during this preliminary research include:

- Additional atmospheric correction efforts are required to understand differences between spectra measured of the same material at the two different spatial resolutions.
- Further studies of spectral variability are required. We need to establish the limits of natural variability for spectral signatures of urban materials as well as limitations imposed by morphology and geometry. The usefulness of image-collected spectral databases on mapping scenes acquired at different times and locations should be examined further.
- Exploration of image segmentation methods to reduce data complexity and improve mapping detail.
- We need to determine improved methods for presentation of mapping results. This includes improved presentation of classification maps, combination of VNIR/SWIR results, and generation of orthorectified map-size products for use in field verification

Some more general suggestions for additional research include:

- Improved spectral characterization of selected materials: this requires collection of additional endmember spectra from the AVIRIS data followed by field verification. We need to identify the materials, characterize their occurrence, and measure field spectra.
- Additional HSI baselining of the urban environment: More detailed studies of the Run 08 and Run 10 data with special attention to spatial resolution effects on spectral identification and mapping.
- Design of spectral databases and population of these databases with spectral measurements of the urban environment and background materials. Generation of metadata and inclusion in the spectral databases.
- Validation and refinement of hyperspectral mapping capabilities utilizing ground truth. This includes collection of site-specific spectral libraries utilizing a field spectrometer and iterative improvements to spectral characterization and mapping with hyperspectral data.
- Extension of the mapping to the full Boulder, Colorado AVIRIS dataset, including image basemap generation (mosaicking), spectral mapping, and ground-truth generation.
- Design and evaluation of approaches and products utilizing combined high-spatial-resolution (panchromatic and multispectral) data with hyperspectral data.

6.0 Acknowledgements

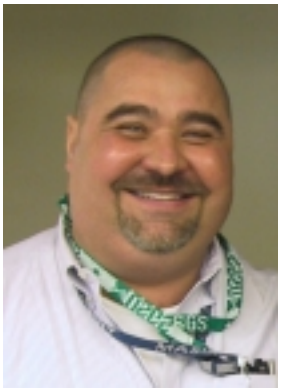

This research is dedicated to the memory of Joseph M. Sadlik (1960 – 2003), a colleague and friend. Joe was instrumental in designing and initiating the Boulder hyperspectral project. His dedication to science and enthusiasm for life will not be forgotten.

7.0 References

Analytical Imaging and Geophysics LLC (AIG), 2001, "ACORN User's Guide, Stand Alone Version," Analytical Imaging and Geophysics LLC, 64 p.

Boardman, J. W., 1998, Leveraging the high dimensionality of AVIRIS data for improved sub-pixel target unmixing and rejection of false positives: mixture tuned matched filtering: in Summaries of the 7th Annual JPL Airborne Geoscience Workshop, JPL Publication 97-21, v. 1, p. 55.

Boardman, J. W., 1999, Precision geocoding of low-altitude AVIRIS data: Lessons learned in 1998: in Summaries of the Eighth Annual JPL Airborne Geoscience Workshop, JPL Publication 99-17, p. 63-68.

Boardman J. W., and Kruse, F. A., 1994, "Automated spectral analysis: A geologic example using AVIRIS data, north Grapevine Mountains, Nevada," in Proceedings, Tenth Thematic Conference on Geologic Remote Sensing, ERIM, Ann Arbor, MI, p. I-407 - I-418.

Boardman, J. W., Kruse, F. A., and Green, R. O., 1995, Mapping target signatures via partial unmixing of AVIRIS data: in Summaries, 5th JPL Airborne Earth Science Workshop, JPL Publication 95-1, 1: 23-26.

Boardman, J. W., 1993, Automated spectral unmixing of AVIRIS data using convex geometry concepts: in Summaries, Fourth JPL Airborne Geoscience Workshop, JPL Publication 93-26, 1: 11 - 14.

Clark, R. N., King, T. V. V., Klejwa, M., and Swayze, G. A, 1990, "High spectral resolution spectroscopy of minerals," Journal of Geophysical Research, v. 95, no. B8, p. 12653-12680.

Clark, R. N., Gregg A. Swayze, K. Eric Livo, Raymond F. Kokaly, Steve J. Sutley, J. Brad Dalton, Robert R. McDougal, and Carol A. Gent, 2003, Imaging spectroscopy: Earth and planetary remote sensing with the USGS Tetracorder and expert systems: Journal of Geophysical Research, V. 108, No E12, p. 5-1 to 5-44.

Fiumi, L., 2001, Evaluation of MIVIS hyperspectral data for mapping covering materials in the urban areas: in Proceedings of the IEEE/ISPRS Joint Workshop on Remote Sensing and Data Fusion over Urban Areas, Rome, Italy, November 8-9th, 2001.

Goetz, A. F. H., G. Vane, J. E. Solomon, and B. N. Rock, 1985, "Imaging spectrometry for earth remote sensing," Science, v. 228, p. 1147 – 1153.

Green, A. A., Berman, M., Switzer, B., and Craig, M. D., 1988, A transformation for ordering multispectral data in terms of image quality with implications for noise removal: IEEE Transactions on Geoscience and Remote Sensing 26 (1): 65 - 74.

Heiden, U., S. Roessner, K. Seg, H. Kaufmann, 2001, Analysis of spectral signatures of urban surfaces for their area-wide identification using hyperspectral HyMap data: in Proceedings of the IEEE/ISPRS Joint Workshop on Remote Sensing and Data Fusion over Urban Areas, Rome, Italy, November 8-9th, 2001

Kruse, F. A., and Lefkoff, A. B., 1993, "Knowledge-based geologic mapping with imaging spectrometers," Remote Sensing Reviews, Special Issue on NASA Innovative Research Program (IRP) results, v. 8, p. 3 – 28.

Kruse, F. A., Boardman, J. W., and Huntington, J. F., 1999, Fifteen Years of Hyperspectral Data: northern Grapevine Mountains, Nevada: in Proceedings of the 8th JPL Airborne Earth Science Workshop: Jet Propulsion Laboratory Publication, JPL Publication 99-17, p. 247 – 258.

Kruse, F. A., Lefkoff, A. B., and Dietz, J. B., 1993a, Expert System-Based Mineral Mapping in northern Death Valley, California/Nevada using the Airborne Visible/Infrared Imaging Spectrometer (AVIRIS): Remote Sensing of Environment, Special issue on AVIRIS, May-June 1993, v. 44, p. 309 - 336.

Kruse, F. A., Lefkoff, A. B., Boardman, J. B., Heidebrecht, K. B., Shapiro, A. T., Barloon, P. J., and Goetz, A. F. H., 1993b, The Spectral Image Processing System (SIPS) - Interactive Visualization and Analysis of Imaging Spectrometer Data: Remote Sensing of Environment, Special issue on AVIRIS, May-June 1993, 44: 145 - 163.

Kruse, F. A., Boardman, J. W., and Huntington, J. F., 2003, Evaluation and Validation of EO-1 Hyperion for Mineral Mapping: in Special Issue, Transactions on Geoscience and Remote Sensing (TGARS), IEEE, v. 41, no. 6, June, p. 1388 – 1400.

Kruse, F. A., Richardson, L.L., and Ambrosia, V. G., 1997, Techniques developed for geologic analysis of hyperspectral data applied to near-shore hyperspectral ocean data: In Proceedings, ERIM 4th International Conference, Remote Sensing for Marine and Coastal Environments: Environmental Research Institute of Michigan (ERIM), Ann Arbor, v. I, p. I-233 - I-246.

Kruse, F. A., 2003, Preliminary Results – Hyperspectral mapping of coral reef systems using EO-1 Hyperion, Buck Island, U.S. Virgin Islands: In proceedings 12th JPL Airborne Geoscience Workshop, Jet Propulsion Laboratory, 24 –28 February 2003, Pasadena, CA (in press)

Kruse, F. A., 2004, Comparison of ATREM, ACORN, and FLAASH atmospheric corrections using low-altitude AVIRIS data of Boulder, Colorado: in Proceedings of the 2004 AVIRIS Earth Science and Applications Workshop, 31 March – 2 April 2004, Jet Propulsion Laboratory Publication (in press – this volume)

Marino, C. M., C. Panigada, L. Busetto, 2001, Airborne Hyperspectral Remote Sensing applications in Urban Areas: Asbestos Concrete Sheeting Identification and Mapping: in Proceedings of the IEEE/ISPRS Joint Workshop on Remote Sensing and Data Fusion over Urban Areas, Rome, Italy, November 8-9th, 2001.

Research Systems Inc(RSI), 2003, ENVI User's Guide, ENVI Version 4.0, September 2003: Research Systems Inc, 1084 p.